Academic Education Publishing House
Industry Science and Engineering Vol. 1 No. 12, 2024

Large-scale Synthesis of TiO_2 Nanospindle by Liquid Phase Method for Photocatalytic Sewage Treatment

Jinjun Gao, Yongming Fu*
College of Physics and Electronic Engineering, Shanxi University, Taiyuan, Shanxi, China
** Corresponding Author.*

Abstract: This paper reports a liquid-phase method for the large-scale synthesis of TiO_2 nanospindles and evaluates their application in photocatalytic wastewater treatment. By optimizing the synthesis parameters, TiO_2 nanospindles with high crystallinity, mesoporous structure, and large specific surface area have been successfully prepared. The synthesized nanospindles are thoroughly characterized. Photocatalytic experiments show that TiO_2 nanospindles effectively degrade methylene blue under UV light, achieving near-complete degradation in 15 minutes. Photoluminescence spectroscopy revealed a high recombination rate of photogenerated carriers, indicating the need for further nanostructure optimization to enhance photocatalytic efficiency. This research offers novel perspectives for creating effective materials in wastewater treatment. This study explores the synthesis of TiO_2 nanospindles via a liquid-phase method and their application in photocatalysis for wastewater treatment.

Keywords: TiO_2 Nanospindles; Liquid-Phase Synthesis; Photocatalysis; Wastewater Treatment

1. Introduction

Water pollution is a major global environmental issue, primarily caused by the rising release of untreated or insufficiently treated wastewater from industrial, agricultural, and domestic activities [1]. Contaminants in sewage, including organic pollutants, heavy metals, and pathogens, pose significant risks to human health and ecosystems [2]. For instance, organic pollutants such as dyes, pharmaceuticals, and pesticides can accumulate in aquatic environments, disrupting ecosystems and entering the food chain. Heavy metals like lead, mercury, and cadmium are toxic even at low concentrations and can cause severe health problems, including neurological damage and cancer. Pathogens in untreated sewage can lead to waterborne diseases, affecting millions of people annually, particularly in developing regions.

Traditional sewage treatment methods, such as activated sludge processes and chemical coagulation, have been widely used for decades. However, these methods often fail to effectively remove complex organic pollutants, particularly those that are resistant to biodegradation or chemical breakdown. This limitation has necessitated the development of advanced treatment technologies capable of addressing these persistent contaminants. Photocatalysis has gained significant interest for its capacity to utilize solar energy in degrading organic pollutants, providing a sustainable approach to wastewater treatment [3-5]. Photocatalysis involves using light to activate a catalyst, which accelerates chemical reactions to decompose pollutants into less harmful substances. This method is attractive due to its use of sunlight, a renewable energy source, which ensures environmental sustainability and long-term cost-effectiveness. TiO_2 is a semiconductor material that exhibits remarkable photocatalytic properties under ultraviolet (UV) light irradiation. When exposed to light, TiO_2 forms electron-hole pairs that react with water and oxygen, creating reactive species like hydroxyl radicals (•OH) and superoxide anions ($•O_2^-$). Reactive species are essential in oxidatively degrading organic pollutants, converting them into less harmful substances. The photocatalytic efficiency of TiO_2 is significantly affected by its morphology, crystallinity, and surface area [6-8]. Recent studies have demonstrated that specific nanostructures, such as nanospindles, can enhance photocatalytic performance by

providing a larger surface area for adsorption and facilitating charge separation, thereby reducing the recombination rates of electron-hole pairs. However, existing TiO_2 synthesis techniques typically rely on organo-titanium compounds such as titanium tetrabutoxide or titanium isopropoxide, which pose significant challenges for large-scale synthesis due to their high cost and complexity [9,10].

In this study, a liquid-phase method for the large-scale synthesis of TiO_2 nanospindles has been developed, which offers advantages of high cost-effectiveness and scalability. By optimizing the synthesis parameters, TiO_2 nanospindles are synthesized with controlled morphology and properties, suitable for photocatalytic applications. The synthesized nanospindles are thoroughly characterized by several techniques to confirm their structural integrity and morphology. Furthermore, the photocatalytic activity of TiO_2 nanospindles is evaluated for the degradation of organic pollutants under ultraviolet light irradiation. The findings will clarify the link between TiO_2's structural features and its photocatalytic efficiency, facilitating the creation of effective wastewater treatment materials.

2. Experiment

2.1 Synthesis of TiO2 Nanospindles

TiO_2 nanospindles were synthesized via a liquid-phase method. 8 g of titanium sulfate was dissolved in 100 mL of deionized water and stirred for 60 minutes to form a 0.5 M transparent solution. Ammonia solution was then gradually added under continuous stirring until the pH reached 9, producing a titanium oxoacid precipitate suspension. The precipitate was rinsed thrice with deionized water to eliminate impurities, resulting in 5.8 g of titanium oxoacid. Next, 11.6 g of a 30 wt% hydrogen peroxide solution was added to the titanium oxoacid precipitate, maintaining a mass ratio of hydrogen peroxide to titanium oxoacid of 2:1. The mixture was stirred until a transparent yellow titanium peroxide precursor formed. A 50% hydroxylamine solution (0.165 g) was added to the titanium peroxide precursor and stirred for 60 minutes at 25°C. This method can realize the synthesis of tons of TiO_2 nanocrystals.

2.2 Characterization

The synthesized TiO_2 nanospindles were characterized using several techniques to evaluate their structural, morphological, and optical properties. X-ray diffraction (XRD) was employed to determine the crystalline phase and structure. Transmission electron microscopy (TEM) offered comprehensive insights into morphology and particle size distribution. The specific surface area and pore structure were assessed using Brunauer–Emmett–Teller (BET) analysis. UV–Vis diffuse reflectance spectroscopy (UV–VIS DRS) was used to investigate the optical absorption properties. Fourier-transform infrared spectroscopy (FTIR) was utilized to detect functional and surface hydroxyl groups. Photoluminescence spectroscopy was employed to assess the recombination rate of photogenerated carriers. X-ray photoelectron spectroscopy (XPS) analyzed the surface's elemental composition and chemical states.

2.3 Photocatalytic Test

The photocatalytic performance of TiO_2 nanospindles was assessed through the degradation of MB under UV light exposure. A 40 mL MB solution (5 mg L^{-1}) was stirred in the dark for 30 minutes in a photocatalytic device to achieve adsorption-desorption equilibrium. The 365 nm UV light source was then activated to initiate the photocatalytic reaction. Liquid samples were collected every 3 minutes, centrifuged to remove TiO_2 catalysts, and analyzed using a UV–Vis spectrophotometer to measure MB degradation based on absorbance at 664 nm.

3. Results and Discussion

The XRD pattern of the TiO_2 sample (Figure 1a) offers a comprehensive understanding of the material's crystallographic structure and phase purity, which are critical factors for its photocatalytic performance. The sharp and well-defined diffraction peaks observed at specific 2θ angles of 25.28°, 37.96°, 47.92°, 54.22°, 62.73°, 69.06°, and 75.22° are indicative of a highly crystalline structure. These peaks correspond to the anatase TiO_2 crystal planes of (101), (004), (200), (105), (204), (116), and (215). The anatase phase is particularly advantageous for photocatalytic applications due to its superior charge carrier mobility and lower electron-hole

recombination rates compared to other TiO_2 polymorphs such as rutile or brookite. The XRD pattern's lack of extraneous peaks verifies the phase purity of the synthesized TiO_2 sample, indicating the material is devoid of impurities or secondary phases that might impair its photocatalytic efficiency. The material's high crystallinity and phase purity are crucial for optimizing its performance in applications like water splitting, pollutant degradation, and solar energy conversion.

Complementing the XRD analysis, the TEM image (Figure 1b) provides detailed insights into the morphology of the TiO_2 sample, revealing spindle-shaped nanocrystals, or "nanospindles", which are characterized by their thicker central region and tapered ends. This distinctive morphology is advantageous for photocatalysis, providing a large surface area for reactant adsorption and potentially improving light absorption due to its anisotropic structure. The high-resolution TEM image (Figure 1c) provides additional structural details of the nanospindles, indicating an average length of 15 nm and a width of 7 nm. The 0.34 nm lattice fringe spacing, indicative of the anatase TiO_2 (101) crystal plane, confirms the material's high crystallinity as supported by XRD results. The well-defined lattice fringes observed in the TEM image also indicate a low density of structural defects, which is crucial for minimizing electron-hole recombination during photocatalytic processes. This reduction in recombination rates is vital for enhancing the overall efficiency of the photocatalytic reactions.

Moreover, the selected-area electron diffraction (SAED) pattern (Figure 1d) provides a direct visualization of the crystallographic planes, further validating the findings from the XRD and TEM analyses. The ring-like pattern in the SAED image corresponds to the diffraction planes of anatase TiO_2, consistent with the XRD data. This agreement between the XRD, TEM, and SAED results reinforces the conclusion that the TiO_2 sample is highly crystalline and phase-pure, with a well-defined anatase structure. The combination of these analytical techniques not only confirms the structural integrity of the TiO_2 nanospindles but also highlights their potential for high-performance photocatalytic applications. The synergistic effect of high crystallinity, phase purity, and unique morphology makes these TiO_2 nanospindles a promising candidate for advanced photocatalytic systems, where efficient charge separation and light absorption are paramount.

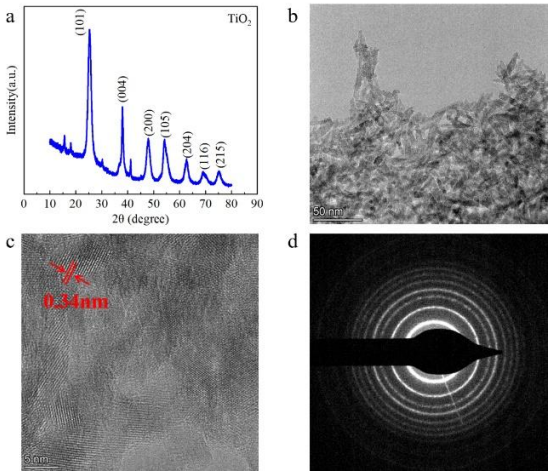

Figure 1. Structural Analyses of TiO_2 Nanospindles. (a) XRD Pattern of TiO_2. (b) TEM Image of TiO_2. (c) High-resolution TEM Image. (d) SAED Pattern.

The XPS survey spectrum (Figure 2a) presents an elemental analysis of the TiO_2 sample, identifying three peaks at 530 eV (O1s), 459 eV (Ti2p), and 285 eV (C1s). These peaks align with the expected composition of TiO_2, where the O1s and Ti2p peaks are intrinsic to the material, while the C1s peak is likely attributed to surface contamination from ambient exposure or residual organic species, a common occurrence in XPS analysis due to the sensitivity of the technique to surface conditions. The Ti2p spectrum (Figure 2b) is resolved into two distinct peaks at 464.56 eV ($Ti2p_{1/2}$) and 458.68 eV ($Ti2p_{3/2}$), exhibiting a spin-orbit splitting of 5.88 eV. This splitting is characteristic of Ti in the +4 oxidation state, confirming the presence of Ti^{4+} in the TiO_2 structure. The absence of peaks corresponding to lower oxidation states (e.g., Ti^{3+}) further supports the high purity and stability of the TiO_2 sample, which is critical for maintaining its photocatalytic performance. The O1s spectrum (Figure 2c) is resolved into two distinct peaks at 529.95 eV and 531.65 eV. The 529.95 eV peak corresponds to lattice oxygen in the TiO_2 framework, crucial for the material's structural integrity. The 531.65 eV peak is linked to surface hydroxyl groups (–OH), which are crucial in photocatalysis.

These hydroxyl groups serve as active sites for adsorbing water molecules and organic pollutants, thereby facilitating surface reactions essential for photocatalytic degradation. The presence of these groups also enhances the hydrophilicity of the TiO_2 surface, which can improve its interaction with aqueous reactants. The combination of lattice oxygen and surface hydroxyl groups highlights the dual role of oxygen in both structural stability and catalytic activity.

The FTIR spectrum (Figure 2d) provides complementary information about the surface chemistry and bonding environment of the TiO_2 sample. The peaks at 3208 cm^{-1} and 1633 cm^{-1} correspond to the stretching and bending vibrations of the O–H bond, respectively. These vibrations are associated with adsorbed water molecules and surface hydroxyl groups, which are consistent with the O1s XPS results. These groups enhance photocatalysis by generating reactive oxygen species (ROS) like hydroxyl radicals, which effectively degrade organic pollutants. The peak at 1398 cm^{-1} is assigned to the bending vibration of the C–H bond, likely arising from residual organic species or carbonaceous contaminants adsorbed on the TiO_2 surface. This observation aligns with the C1s peak in the XPS survey spectrum and suggests that the sample may have been exposed to organic compounds during synthesis or handling. While these contaminants do not significantly affect the bulk properties of TiO_2, they may influence surface reactions and should be considered in photocatalytic applications.

The broad peak observed in the 400–800 cm^{-1} range corresponds to the stretching vibrations of Ti–O–Ti bonds within the TiO_2 lattice. This verifies the TiO_2 structure formation, aligning with the anatase phase observed in XRD and TEM analyses. The FTIR results, combined with the XPS data, provide a comprehensive understanding of the chemical and structural properties of the TiO_2 sample. Surface hydroxyl groups, lattice oxygen, and Ti–O–Ti bonds highlight the material's potential for photocatalytic use, emphasizing its surface reactivity and structural stability. The synergistic insights from XPS and FTIR analyses not only validate the high purity and crystallinity of the TiO_2 sample but also highlight its potential for efficient photocatalytic performance in environmental and energy-related applications.

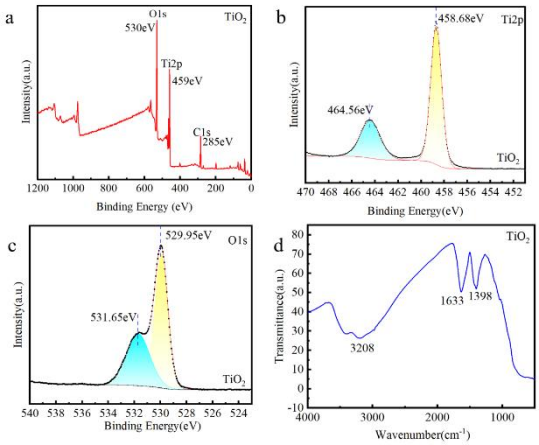

Figure 2. Spectral Analyses of TiO_2 Nanospindles. (a) XPS Survey Spectrum. (b) Ti2p Spectrum. (c) O1s Spectrum. (d) FITR Spectrum.

The N_2 adsorption-desorption isotherm analysis provides critical information about the textural properties of the TiO_2 sample, including its surface area, pore size distribution, and porosity, as shown in Figure 3. The TiO_2 sample displays a type-IV curve with an H2 hysteresis loop, indicative of a mesoporous structure featuring narrow necks linked to larger cavities. This type of hysteresis indicates that the TiO_2 sample has a well-defined mesoporous structure, which is advantageous for photocatalysis. Mesopores improve reactant and product diffusion, increasing active site accessibility. The BET surface area of the TiO_2 sample is 245.1522 $m^2\ g^{-1}$ (Figure 3a), displaying an average pore size of 4.89 nm (Figure 3b). The unique nanospindle morphology, as observed in TEM analysis, contributes to the high surface area, offering increased active sites for reactant adsorption and reactive oxygen species generation. Mesoporous pore sizes optimize photocatalysis by facilitating efficient reactant mass transport and preserving high surface area.

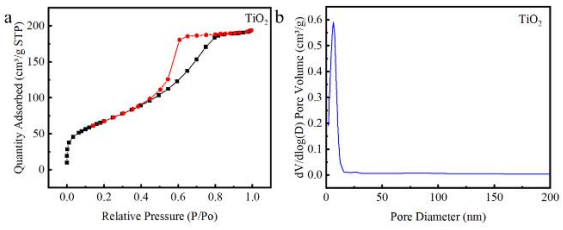

Figure 3. Specific Surface Area of TiO_2 Nanospindles. (a) N_2 Adsorption–Desorption Isotherm. (b) Pore Size Distribution.

The UV–Vis DRS spectrum (Figure 4a) shows that the TiO_2 sample has strong absorption in the ultraviolet (UV) region, with a sharp absorption edge around 410 nm. This is consistent with the intrinsic bandgap of anatase TiO_2 (~3.2 eV). The strong UV absorption results from electron excitation from the valence to the conduction band under UV light, crucial for electron-hole pair generation and photocatalytic reactions. The sample's minimal absorption in the visible spectrum diminishes its photocatalytic efficiency under natural sunlight. The PL spectrum (Figure 4b) shows a broad emission peak between 460–600 nm, suggesting a high recombination rate of photogenerated carriers. This recombination reduces the availability of electrons and holes for generating reactive oxygen species, which are essential for degrading organic pollutants. This suggests that further optimization of the TiO_2 nanostructure may be necessary to reduce recombination and enhance photocatalytic efficiency.

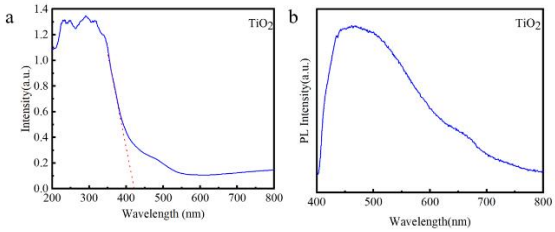

Figure 4. Optical Spectra of TiO_2 Nanospindles. (a) UV-Vis DRS of TiO_2. (b) PL Spectrum of TiO_2.

Figure 5. illustrates the MB degradation curve over time, highlighting the photocatalytic efficiency of the TiO_2 sample under UV light exposure. The MB solution's initial absorbance of 0.98 is used as the baseline to assess degradation efficiency. The absorbance decreases sharply to 0.68 within the first 3 minutes, indicating a rapid onset of photocatalytic activity. This trend continues, with the absorbance dropping to 0.30 after 6 minutes, 0.09 after 9 minutes, and 0.02 after 12 minutes. Upon exposure to UV light for 15 minutes, the final absorbance reaches 0.01, nearly the absorbance intensity of pure water.

The significant and consistent reduction in absorbance over time highlights the efficient degradation of MB. The near-complete degradation achieved within 15 minutes underscores the high photocatalytic activity of the TiO_2 sample. The swift degradation indicates that the TiO_2 catalyst efficiently produces reactive oxygen species, such as hydroxyl and superoxide radicals, under UV light irradiation. These ROS are highly reactive and play a critical role in breaking down MB molecules into smaller, less harmful compounds, such as carbon dioxide and water. The rapid generation of ROS is facilitated by the high crystallinity and phase purity of the anatase TiO_2, as confirmed by XRD and TEM analyses, which minimize electron-hole recombination and enhance charge carrier mobility.

The excellent photocatalytic performance of the TiO_2 sample can be attributed to several factors. First, the unique spindle-shaped morphology of the TiO_2 nanocrystals provides a high surface area, which increases the availability of active sites for pollutant adsorption and photocatalytic reactions. Second, the anatase phase of TiO_2 is known for its superior photocatalytic properties compared to other phases, such as rutile or brookite, due to its optimal bandgap energy and efficient charge separation. Third, the presence of surface hydroxyl groups, as identified by XPS and FTIR analyses, further enhances photocatalytic activity by promoting the adsorption of water molecules and facilitating the generation of ROS.

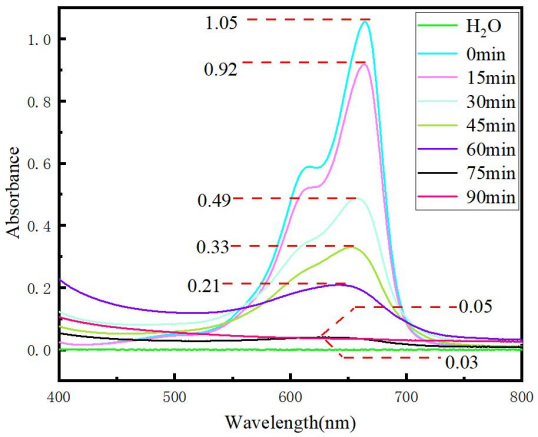

Figure 5. Photocatalytic Degradation of MB.

The TiO_2 sample's ability to effectively degrade organic pollutants such as MB demonstrates its potential for practical applications in wastewater treatment and environmental remediation. For instance, it could be used to remove organic dyes, pharmaceuticals, and other hazardous pollutants from industrial effluents. Additionally, the material's high stability and

reusability make it a cost-effective and sustainable solution for large-scale environmental applications. Future studies could explore the optimization of synthesis parameters to further enhance photocatalytic efficiency or investigate the performance of TiO_2 under visible light to broaden its applicability in solar-driven photocatalytic systems. Overall, the results highlight the TiO_2 sample as a promising candidate for addressing environmental challenges through advanced photocatalytic technologies.

4. Conclusion

In this study, we have successfully synthesized TiO_2 nanospindles using a cost-effective and scalable liquid-phase method. The synthesized TiO_2 demonstrated high crystallinity, mesoporosity, and an extensive surface area, rendering it suitable for photocatalytic applications. The PL spectrum indicates a high recombination rate of photogenerated carriers, highlighting the need for further optimization to improve photocatalytic efficiency. Future work will focus on modifying the TiO_2 nanostructure to reduce recombination and improve visible light absorption, paving the way for more efficient photocatalytic materials for wastewater treatment.

Acknowledgement

This work was supported by the Shanxi Province Graduate Student Research Innovation Project (Grant No.2024KY102), and the Xinzhou Key Research and Development Project (Grant No.20240102).

References

[1] Seul-Yi Lee, Soo-Jin Park. TiO_2 photocatalyst for water treatment applications. Journal of Industrial and Engineering Chemistry, 2013, 19 (6): 1761-1769.

[2] Hugues Kamdem Paumo, Sadou Dalhatou, Lebogang Maureen Katata-Seru, et al. TiO_2 assisted photocatalysts for degradation of emerging organic pollutants in water and wastewater. Journal of Molecular Liquids, 2021, 331: 115458.

[3] Dongjie Chen, Yanling Cheng, Nan Zhou, et al. Photocatalytic degradation of organic pollutants using TiO_2-based photocatalysts: A review. Journal of Cleaner Production, 2020, 268 (20): 121725.

[4] Abir Chakravorty, Somnath Roy. A review of photocatalysis, basic principles, processes, and materials. Sustainable Chemistry for the Environment, 2024, 8: 100155.

[5] Nur Hidayatul Syazwani Suhaimi, Rahil Azhar, Nur Syamimi Adzis, et al. Recent updates on TiO_2-based materials for various photocatalytic applications in environmental remediation and energy production. Desalination and Water Treatment, 2025, 321: 100976.

[6] Zhinuo Wang, Shimin Liu, Xin Cao, et al. Preparation and characterization of TiO_2 nanoparticles by two different precipitation methods. Ceramics International, 2020, 46 (10): 15333-15341.

[7] M.M. Viana, V.F. Soares, N.D.S. Mohallem. Synthesis and characterization of TiO_2 nanoparticles. Ceramics International, 2010, 36(7): 2047-2053.

[8] Sukarman, Budi Kristiawan, Khoirudin, et al. Characterization of TiO_2 nanoparticles for nanomaterial applications: Crystallite size, microstrain and phase analysis using multiple techniques. Nano-Structures & Nano-Objects, 2024, 38: 101168.

[9] K. Prajapat, U. Mahajan, M. Dhonde, et al. Synthesis and characterization of TiO_2 nanoparticles: Unraveling the influence of copper doping on structural, surface morphology, and optical properties. Chemical Physics Impact, 2024, 8: 100607.

[10] William Bang Lomholdt, Matthew Helmi Leth Larsen, Cuauhtemoc Nuñez Valencia, et al. Interpretability of high-resolution transmission electron microscopy images. Ultramicroscopy, 2024, 263: 113997.